LBL-35596
UC-413

Lawrence Berkeley Laboratory
UNIVERSITY OF CALIFORNIA

Presented at the International Workshop on Dynamical Features of Nuclei and Finite Fermi Systems, Sitges, Barcelona, Spain, September 13–17, 1993, and to be published in the Proceedings

Collective Flow and Azimuthal Correlations in Nucleus-Nucleus Collisions at the Bevalac

G. Rai and the EOS Collaboration

September 1993

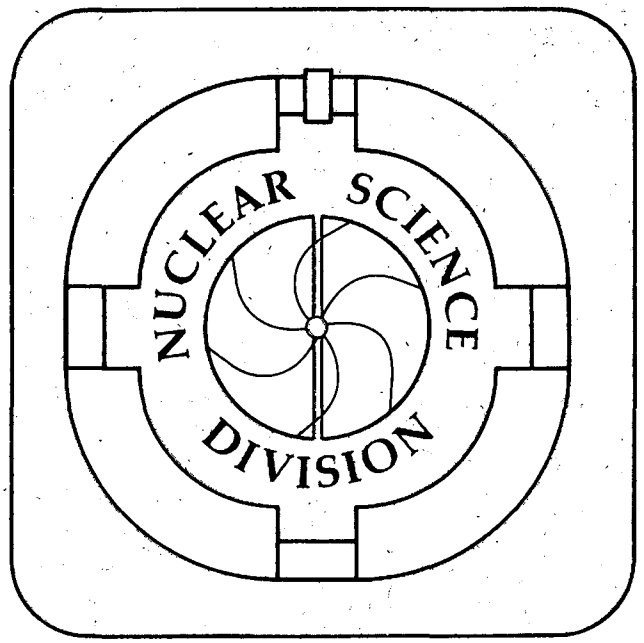

Prepared for the U.S. Department of Energy under Contract Number DE-AC03-76SF00098

DISCLAIMER

LBL-35596
UC-413

Collective Flow and Azimuthal Correlations in Nucleus-Nucleus Collisions at the Bevalac

S. Albergo,[7] F. Bieser,[1] F.P. Brady,[4] Z. Caccia,[7] D. Cebra,[4] A.D. Chacon,[5] J. Chance,[4] Y. Choi,[8] S. Costa,[7] J. Elliott,[3] M. Gilkes,[3] A. Hauger,[3] A. Hirsch,[3] E. Hjort,[3] A. Insolia,[7] M. Justice,[2] D. Keane,[2] V. Lindenstruth,[6] H.S. Matis,[1] M. McMahan,[1] C. McParland,[1] W.F.J. Müller,[6] D.L. Olson,[1] M.D. Partlan,[4] N. Porile,[3] R. Potenza,[7] G. Rai,[1] J. Rasmussen,[1] H.G. Ritter,[1] J. Romanski,[7] J.L. Romero,[4] G.V. Russo,[7] H. Sann,[6] R. Scharenberg,[3] A. Scott,[2] Y. Shao,[2] B. Srivastava,[3] T.J.M. Symons,[1] M. Tincknell,[3] C. Tuve,[7] S. Wang,[2] P. Warren,[3] H. Wieman,[1] and K. Wolf[5]

[1]Lawrence Berkeley Laboratory, Berkeley, California 94720
[2]Kent State University, Kent, Ohio 44242
[3]Purdue University, West Lafayette, Indiana 47907-1396
[4]University of California, Davis, California 95616
[5]Texas A&M, College Station, Texas 77843
[6]Gesellschaft für Schwerionenforschung, Darmstadt, Germany, D-64220
[7]Universita' di Catania & INFN-Sezione di Catania, Catania, Italy, 95129
[8]Sung Kwun Kwan University, Suwon, Rep. of Korea, 440-746

September 1993

This work was supported by the Director, Office of Energy Research, Office of High Energy and Nuclear Physics, Division of Nuclear Physics of the U.S. Department of Energy under Contract No. DE-AC03-76SF00098.

Collective Flow and Azimuthal Correlations in Nucleus-Nucleus Collisions at the Bevalac

G. Rai and the EOS Collaboration:

S. Albergo,[7] F. Bieser,[1] F. P. Brady,[4] Z. Caccia,[7] D. Cebra,[4]
A. D. Chacon,[5] J. Chance,[4] Y. Choi,[8] S. Costa,[7] J. Elliott,[3]
M. Gilkes,[3] A. Hauger,[3] A. Hirsch,[3] E. Hjort,[3] A. Insolia,[7]
M. Justice,[2] D. Keane,[2] V. Lindenstruth,[6] H. S. Matis,[1] M. McMahan,[1]
C. McParland,[1] W. F. J. Müller,[6] D. L. Olson,[1] M. D. Partlan,[4] N. Porile,[3]
R. Potenza,[7] G. Rai,[1] J. Rasmussen,[1] H. G. Ritter,[1] J. Romanski,[7]
J. L. Romero,[4] G. V. Russo,[7] H. Sann,[6] R. Scharenberg,[3] A. Scott,[2]
Y. Shao,[2] B. Srivastava,[3] T. J. M. Symons,[1] M. Tincknell,[3] C. Tuve,[7]
S. Wang,[2] P. Warren,[3] H. Wieman,[1] K. Wolf [5]

[1]Lawrence Berkeley Laboratory, Berkeley, California, 94720
[2]Kent State University, Kent, Ohio 44242
[3]Purdue University, West Lafayette, Indiana, 47907-1396
[4]University of California, Davis, California, 95616
[5]Texas A&M, College Station, Texas, 77843
[6]Gesellschaft für Schwerionenforschung, Darmstadt, Germany, D-64220
[7]Universita' di Catania & INFN-Sezione di Catania, Catania, Italy, 95129
[8]Sung Kwun Kwan University, Suwon, Rep. of Korea, 440-746

Abstract

The EOS experiment at the Bevalac has recently carried out exclusive event-by-event measurements of relativistic heavy ion collisions with a variety of projectile, target and beam energy combinations. The data was obtained using the EOS Time Projection Chamber. We present preliminary results on inclusive spectra, collective flow and azimuthal correlations obtained from a study of Au+Au reactions with beam energies covering 0.6 - 1.2 A GeV.

1 Introduction

Past experiments [1, 2] have proven collective flow exists in high energy heavy ion collisions. Different aspects have been identified (bounce-off, side-splash, and squeeze-out) and their mass and energy dependence have been studied. Flow effects resulting from nuclear compression are known to depend on both the static, that is, the equation of state (EOS), and the dynamic properties of the collision. Progress towards an understanding of the nuclear matter EOS has been slow. This is due in part to the uncertainties in the theoretical description of the collision dynamics, for example, the pronounced influence of in-medium effects and momentum-dependent interactions on the EOS. Experience has shown that it might be possible to resolve ambiguities by requiring models to simultaneously describe a comprehensive set of observables that are sensitive to the underlying EOS. Previous exper-

iments lacked the systematics and did not measure most of the signal in a collision event because of detector limitations.

New measurements on relativistic heavy ion collisions have been made at the Bevalac using a 4π detector system, with particle indentification and momentum measurement. High statistics data was obtained with a variety of projectile, target and beam energy combinations listed in table 1. In the first phase of the analysis we have concentrated on the mass and energy dependence of flow in symmetric Au+Au collisions. Our preliminary results are presented in this paper.

Beam Projectile	Incident Energy	Target
Au	0.25 - 1.2 A GeV	Be, C, Al, Ca, Cu, Nb, La, Au, U
La	0.4 - 1.3 A GeV	C, Al
Ni	0.25 - 2.0 A GeV	Be, Cu, Au
Kr	1.0 A GeV	C, Al
Ca	0.8 - 2.1 A GeV	Be, Ca, Au

Table 1: Summary of the data obtained by the EOS Experiment

2 The EOS Experimental Arrangement

The arrangement of detectors are shown schematically in Fig. 1. The apparatus provides substantial phase space coverage in the center of mass system (close-to-4π) with simultaneous particle identification. The principal tracking detector is a sophisticated heavy ion Time Projection Chamber called the EOS TPC [3] which provides continuous three dimensional tracking of charged particles and most of the event characterization. The TPC is located between the pole tips of a large aperture, 1.3T, superconducting dipole magnet, and therefore, particle identification (up to Z $\sim$ 5-6) is obtained from the magnetic rigidity and multiple energy loss measurements along the path of an individual track.

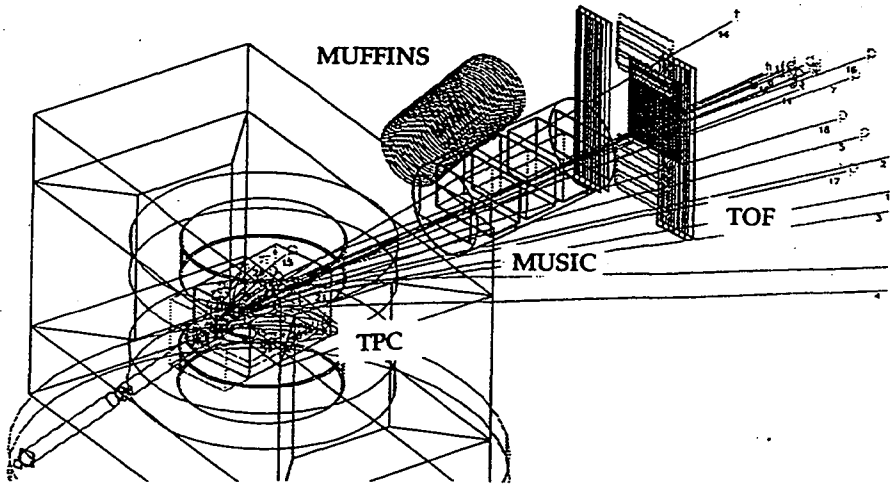

Figure 1: A perspective view of the EOS experimental setup at the Bevalac.

Two detectors called MUSIC and the TOF wall are located downstream of the EOS TPC. MUSIC is a large volume, multiple sampling ionization chamber which measures the trajectory and identifies the charge of heavy fragments ranging from Carbon to beam particles. The TOF wall consists of a movable array of scintillator slats which measures the time of flight of light mass fragments and identifies their element number. The combination of MUSIC and the TOF wall were used to identify the forward going projectile fragments which are beyond the dynamic range of the TPC and thus provide full acceptance for the reverse kinematic experiments. The MUFFINS detector recorded the energy and angular position of the neutrons emitted in the beam direction. The data from all the detectors were combined and used in the offline analysis to reconstruct the collision event-by-event. In the following sections we discuss the results obtained from the EOS TPC detector alone.

3 Inclusive Spectra

The inclusive spectra of midrapidity (-0.1<y<0.1) pions, protons, deuterons and alphas emitted in midcentral, 1.2 A GeV, Au+Au collisions are plotted in Fig. 2. In terms of a single isotropic fireball model, the momentum distribution for emitted particles at midrapidity (y=0) is given in the center of mass by:

$$\frac{dn}{dydm_t} = const. \times \frac{m_t^2}{e^{m_t/T} + d} \quad (1)$$

where d = +1,-1,0 for a Fermi, Bose, or Boltzmann distribution, m_t is the transverse energy equal to $\sqrt{P^{\perp 2} + m^2}$ and T is the temperature.

The solid lines in Fig. 2 represent the fit to the exponential part of Eqn. 1. The inverse slope parameters 1/T are plotted in Fig. 3 as function of particle type and multiplicity bin. In general the slope of the distributions are larger for the more central collisions and heavier mass fragments. The discussion of spectra in terms of a thermal distribution is a gross oversimplication since several complicating factors occur. Any equilibration reached is at best transient and the radial expansion of the system confuses the interpretation of source temperature. The effect of radial hydrodynamic flow on inclusive spectra can be indentified in two extreme cases. If thermal equilibrium is reached, the average kinetic energy of the fragments must be constant and independent of their mass. In the case of hydrodynamic flow, one might assume that each fragment is in motion with the flow velocity. If so, the average kinetic energy is linearly proportional to the mass of the fragment and the source would appear to be hotter. However, an apparently hotter source could also arise from the final state clustering of the nucleons and any collective motion, directed or radial, would merely enhance the effect. A detailed comparison of the data with microscopic models which include dynamical effects, for example Quantum Molecular Dynamics, is in progress.

4 Collective Flow

The global transverse momentum analysis technique developed by Danielwicz and Odyniec [4] was used to measure collective flow. In this method the reaction plane is constructed for each event by summing the transverse momentum components of all particles in the center of mass forward hemisphere and likewise in the backward hemisphere. The difference vector between the two hemispheres, called the Q vector, is an estimate of the reaction

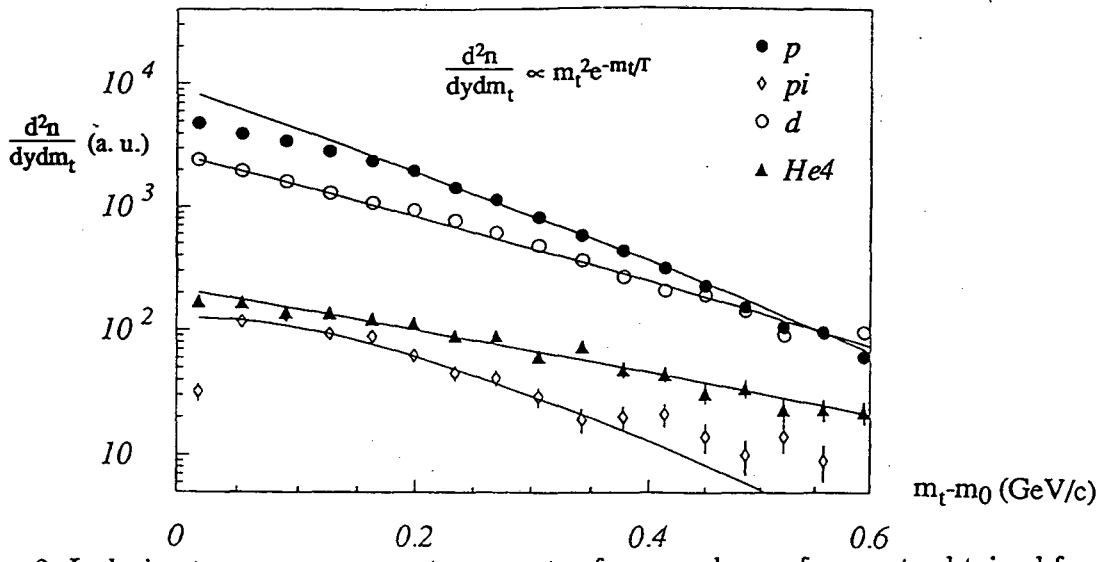

Figure 2: Inclusive transverse momentum spectra for several mass fragments obtained from 1.2 A GeV Au+Au collisions.

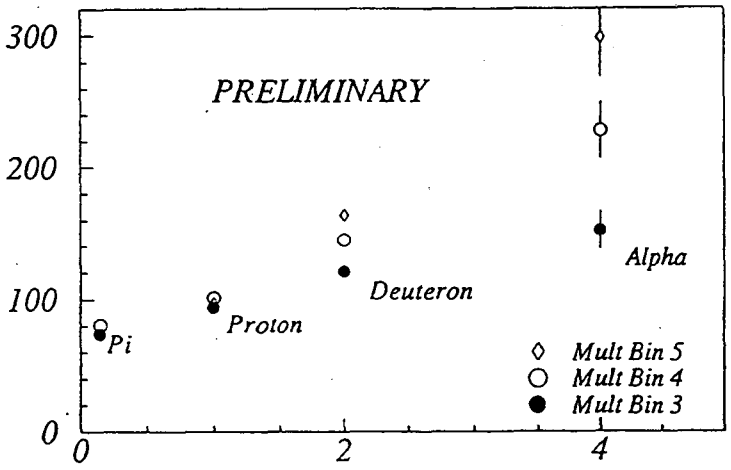

Figure 3: Inverse slope parameters plotted for several mass fragments and multiplicity bins.

plane. Auto–correlation is removed by determining the reaction plane for every fragment by excluding that fragment from the sum:

$$Q = \sum_{i=1}^{n} w(i) P_{\perp}(i) \tag{2}$$

The weights w(i) varied linearly from -1 at target rapidities to $+1$ at projectile rapidities to allow for the fact that fragments near midrapidity are less correlated with the reaction plane.

The transverse momentum vector of each particle is projected onto the reaction plane, yielding the in-plane transverse momentum per nucleon P_x/A, which is subsequently averaged over all events satisfying a multiplicity cut. The rapidity dependence of $\langle P_x/A \rangle$ is shown in Fig. 4 as a function of beam energy. The characteristic S-shape of the emerging curve is a clear sign of nuclear matter flow. The general features of the distributions are: a) particles close to the beam rapidity show maximum directed flow, b) the peak value of $\langle P_x/A \rangle$ is a constant 0.1 GeV/c/A, independent of beam energy above 0.6 A GeV, and c) for the stopped, thermalized particles at mid-rapidity, the transverse momentum $\langle P_x/A \rangle$ van-

ishes. The projectile and spectator regions are observed to behave differently at 1.2 A GeV than at 0.6 A GeV. This effect is not fully understood.

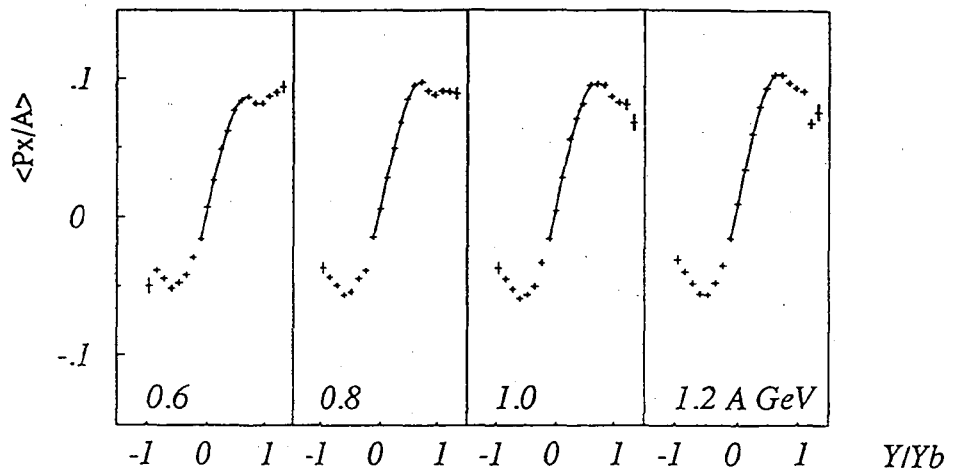

Figure 4: Transverse momentum $\langle P_x/A \rangle$ versus rapidity for Au+Au collisions at several beam energies.

The slope of the "S-shaped" $\langle P_x/A \rangle >$ curve at midrapidity is given by

$$P_x^{slope} = \left(\frac{d < P_x/A >}{d(y/y_{proj})} \right)_{y=y_{cm}} \tag{3}$$

This quantity is unaffected by the spectator fragments and is often used in the literature as a good indicator of collective flow. We have determined P_x^{slope}, for mid-central (Mul3) Au+Au collisions at 0.6, 0.8 1.0 and 1.2 A GeV beam energies. The excitation function is shown in Fig. 5 for fragments with identified charge up to Z=2, albeit the results are dominated by the protons. For comparison with earlier work, the corresponding data from the Plastic Ball group is also illustrated. The EOS results join smoothly with the Plastic Ball data at 0.6 A GeV and extend the measurements to higher energies. The values of P_x^{slope} increase slowly as function of beam energy whereas the 0.8 A GeV Plastic Ball data point might have suggested the onset of saturation.

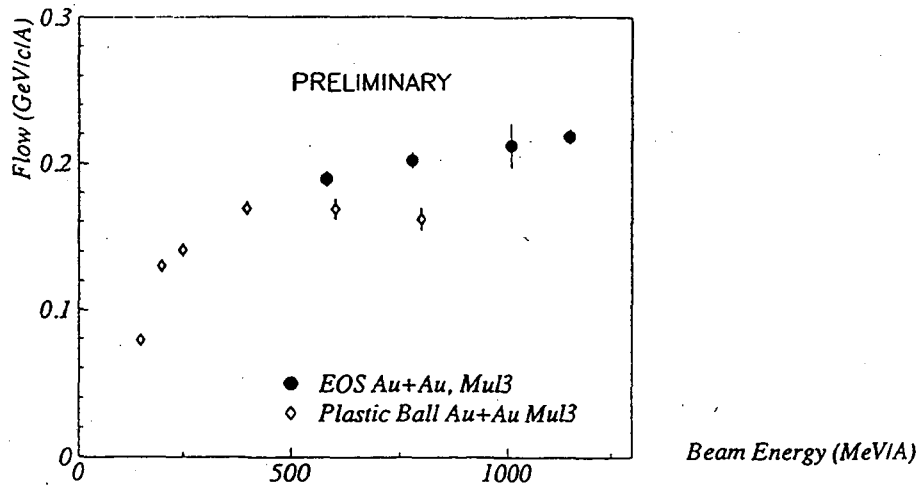

Figure 5: Flow excitation function showing the EOS and Plastic Ball results.

5 Correlations

The azimuthal particle-pair correlation method of Wang et al [5]. was used to study in detail the emission pattern of collective flow. This approach is independent of the reaction plane and, in principle, has the advantage of separating the directed flow correlations into their geometrical and momentum components. The technique relies on the azimuthal angle difference for each fragment pair, defined as $\Phi = |\phi_i - \phi_j|$, where ϕ_i represents the azimuthal angle of the ith fragment. Next one constructs the histogram $dN/d\Phi$ whose functional form should obey:

$$P(\Phi) = \frac{dN}{d\Phi} = A(1 + 0.5\lambda^2 \cos\Phi) \tag{4}$$

where A is a constant normalization factor and λ is related to the azimuthal anisotropy and represents the strength of the collective flow. Adapting the approach of interferometry analysis we define the azimuthal correlation function as:

$$C(\Phi) = \frac{P_{corr}(\Phi)}{P_{uncorr}(\Phi)} \tag{5}$$

where $P_{corr}(\Phi)$ is the measured Φ distribution of pairs in which both fragments are selected from the same event and $P_{uncorr}(\Phi)$ is the Φ distribution for uncorrelated pairs generated by event mixing. Collective flow appears as $C(\Phi) > 1$ at small Φ and as $C(\Phi) < 1$ al large Φ. The magnitude of the observed flow can be quantified by the value of λ in Eqn. 4 that best fits the data for $C(\Phi)$.

In Fig. 6, the correlation function is plotted for 1.2 A GeV Au+Au collisions selected for mid-to-central impact parameters. The data is represented in five rapidity intervals covering the mid-rapidity and beam projectile region. The correlation function develops a stronger $\cos\Phi$ dependence as the intervals approach projectile rapidity. The solid line show the fit used to extract the strength parameter λ, which in turn is plotted in Fig. 7 (left picture) vs. scaled rapidity. Similarly, the values obtained at beam energies of 0.6, 0.8 and 1.0 A GeV are also shown on the same figure. In general, we observe the strength of directed flow is zero at mid-rapidity and increases almost linearly with rapidity. This feature is consistent with the "S-shaped" flow curves shown in the previous section. However, the slope of the strength parameter versus rapidity is essentially independent of beam energy which therefore suggests the azimuthal emission pattern of fragments due to collective flow is also independent of incident beam energy.

We have extended the correlation formalism to investigate the radial part of the directed flow. Specifically, we consider a model in which the directed flow momentum is presumed to be constant. In that case, the measured transverse momentum vector for each fragment can be decomposed into a thermal component, $P^{\perp}_{therm}$, and a part which comes from the directed flow momentum vector, $P^{\perp}_{flow}$, projected along the thermal component. This is not to be confused with the radial or cylindrical flow which might also exist but cannot be studied using the technique described here. Thus, we can write for transverse momentum of the i^{th} fragment:

$$|P^{\perp}_i| = |P^{\perp}_{therm}| + |P^{\perp}_{flow}| \tag{6}$$

Again for each fragment pair we define the sum transverse momentum as

$$|P^{\perp}_{sum}|_{i,j} = |P^{\perp}_i| + |P^{\perp}_j| \tag{7}$$

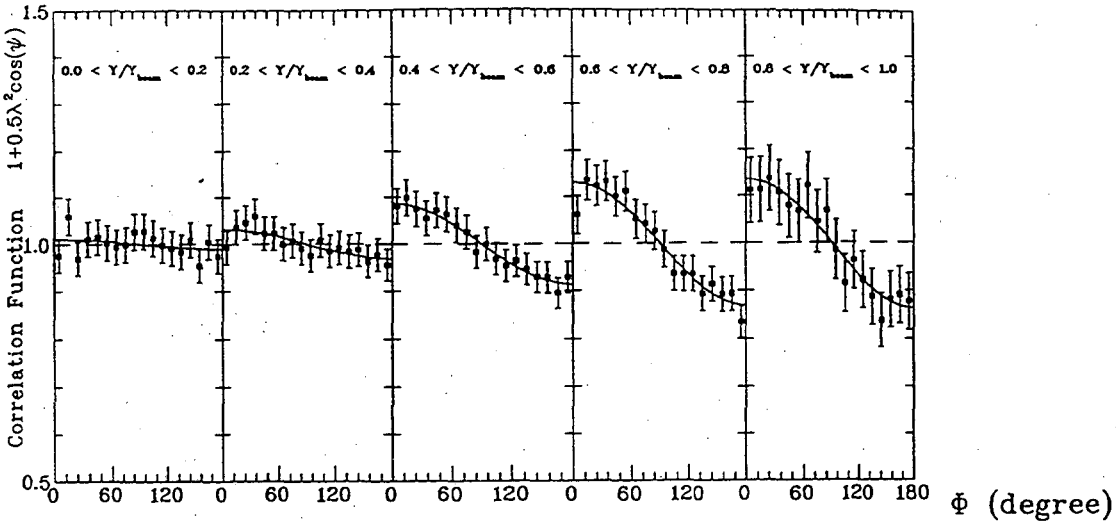

Figure 6: Azimuthal correlation function in several rapidity intervals

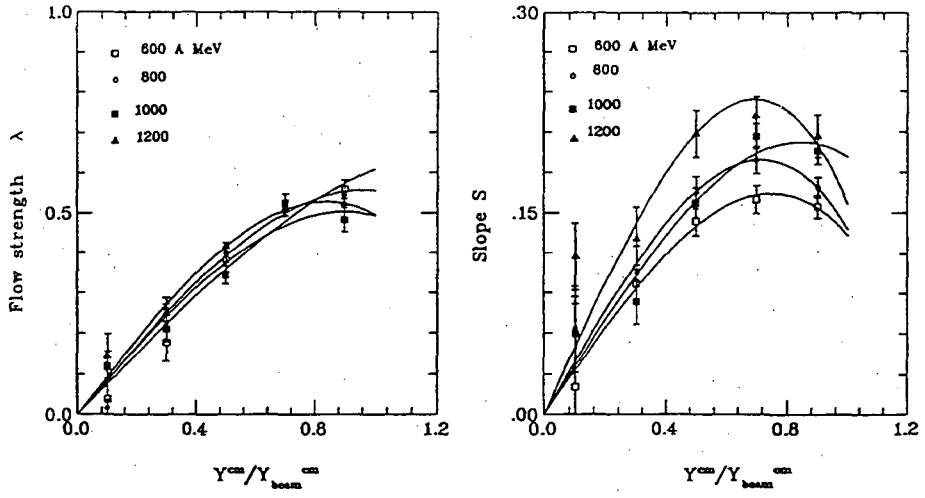

Figure 7: The flow strength parameter, λ, (left) and the slope parameter, S, (right) plotted as a function of rapidity and beam energy.

and its standard deviation by

$$\sigma^2(\Phi) = \langle P_{sum}^{\perp 2} \rangle_{(\Phi)} - \langle P_{sum}^{\perp} \rangle_{(\Phi)}^2 \tag{8}$$

for a given angle difference bin Φ. The averaging is done within a bin. In the absence of flow, a plot of σ^2 vs. Φ should be constant and reflect the width of the thermal background. Collective flow will appear to increase the values of σ^2 by approximately $2(P_{flow}^{\perp})^2$, $P_{flow}^{\perp}$, and 0 for Φ equal to 0°, 90°, and 180° respectively. Thus the slope of σ^2 vs. Φ is measure of the magnitude of directed flow momentum.

In Fig. 8 the value of σ^2 vs. Φ is plotted in five rapidity intervals for Au+Au data at 1.2 A GeV. The slope, S, of the fitted line is steeper for the higher rapidity bins which suggest fragments closer to the projectile rapidity receive a stronger momentum kick from sideward flow. The value of the slopes are plotted in Fig. 7 (right picture) versus rapidity together with the data obtained at the lower beam energies. Unlike the azimuthal correlation function, we observe the gradient of S versus rapidity is enhanced at the higher beam

energies, that is, the directed sideward momentum of fragments becomes stronger with increasing incident beam energy.

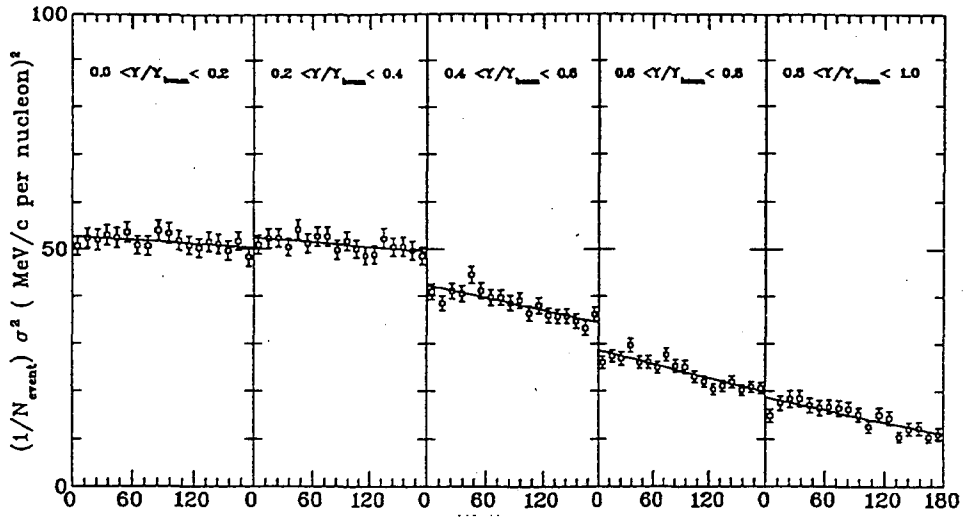

Figure 8: σ^2 versus. Φ in several rapidity intervals

6 Summary

The EOS experiment has obtained extensive data on heavy ion collisions at the Bevalac using the new Time Projection Chamber. We have measured the inclusive spectra for different mass fragments. We find a non-saturating excitation function for sideward directed flow. Azimuthal correlations suggest the emission pattern for directed sideward flow is independent of beam energy while the average flow momentum per nucleon appears to increase at higher beam energies.

This work was supported by the Director, Office of Energy Research, Office of High Energy and Nuclear Physics, Division of Nuclear Physics of the U.S. Department of Energy under Contract DE-AC03-76SF00098.

References

[1] H.H. Gutbrod, et al., Phys. Rev. C42, 640 (1990).
H.A. Gustafsson, et al., Phys. Rev. Lett. 52, 1590 (1984).

[2] D. Beavis et al., Phys. Rev. C45, 299 (1992).
A. Sandoval et al., Nucl. Phys. A400, 365c (1983).

[3] G. Rai, et al., IEEE Trans. Nucl. Sci. 37, 56 (1990).

[4] P. Danielwicz and G. Odyniec, Phys. Lett. 157B, 146, (1985)

[5] S. Wang et al., Phys. Rev. C44, 1091, (1991)

LAWRENCE BERKELEY LABORATORY
UNIVERSITY OF CALIFORNIA
TECHNICAL INFORMATION DEPARTMENT
BERKELEY, CALIFORNIA 94720